Journal of
Mechanical
Science and
Technology

Journal of Mechanical Science and Technology 21 (2007) 924~929

Active Vibration μ-Synthesis-Control of a Hydrostatically Supported Flexible Beam

Peter Kytka*, Christian Ehmann, Rainer Nordmann

Dept. of Mechatronics in Mechanical Engineering, Darmstadt University of Technology, Germany

(Manuscript Received November 16, 2006; Revised January 8, 2007)

Abstract

This paper presents active vibration control of a hydrostatically supported, flexible beam. The objective is to show the capability of active hydrostatic bearings, where the flow rate is controlled with a fast dynamic servo valve. Consequently the damping as well as the stiffness behaviour of the supported structure should be improved. First the damping behaviour is increased by using acceleration feedback in combination with the modern, robust control concept μ-synthesis. It enables to overcome undesirable properties of the mechatronic system as, weakly damped, low frequency flexible modes, phase lag, slight nonlinearities or non-collocation. To increase the stiffness of the bearings the oil gap is used as control variable and controlled to constant with PI-control. Finally, the obtained results are compared with the state-of-the-art technology of hydrostatic bearings.

Keywords: Active vibration control; Hydrostatically supported beam; μ -synthesis

1. Introduction

In recent years active vibration control has been investigated in many kinds of technical applications, (Balas and Doyle, 1994 ; Preumont, 2002). The objective is to reduce undesirable vibrations of a flexible, mechanical structure. These vibrations are generated by disturbing forces, torques, or accelerations. One of the benefits of active vibration control is the dissipation of energy with a small additional actuator weight. This allows to solve the conflict of passive lightweight structures where the mass reduction and a high stiffness leads to a decrease of structural damping. Simultaneously, the static stiffness of the structure is nearly kept constant. Anyhow, for active vibration control higher complexity and costs have to be taken into account.

A variety of actuator principles such as piezoelectric or electromagnetic combined with different control strategies can be used for realisation of active vibration control. Depending on the requirements and the given process, an adequate concept has to be chosen. This paper focuses on active hydrostatic bearings to achieve vibration control of a flexible structure. Thereby forces of defined magnitude and frequency act on the flexible structure and enable the compensation of disturbances. The forces are controlled indirectly by a fast dynamic servo valve, which is used to affect the flow rate of the hydrostatic bearings and hence to improve the stiffness and damping behaviour. To consider system properties as, weakly damped flexible modes, slight nonlinearities, parameter changes or non-collocation the robust control concept μ-synthesis has been applied successfully. Experimental results and theory can be found in Schönhoff (2003) and in the references mentioned there.

Applications of active hydrostatic bearings for vibration control are rarely to be found in literature.

*Corresponding author. Tel.: +49 6151 165607, Fax.: +49 6151 165332
E-mail address: kytka@min.tu-darmstadt.de

Basics and examples about hydrostatic bearings are explained in Weck (2002) and in the references mentioned there. Hesselbach *et al.* (1999, 2002) describe the design of a novel actuator for the control of active hydrostatic bearings with electro-rheological and magneto-rheological fluids as active medium.

2. Active hydrostatic bearings

Active hydrostatic bearings can be used in guide ways for flexible structures, e.g. in axes of machine tools. Appropriate system properties of hydrostatic bearings are, fluid friction only, i.e. no stick-slip-effect, wearless motion and particularly a high damping ratio in the direction of the supported load. The main disadvantages of the hydrostatic principle are high costs and increased complexity for realisation and maintenance.

2.1 Design and function

The principle design and function of a single hydrostatic bearing with a mass m is depicted in Fig. 1. Beneath the mass, the slide surface of the guide has an integrated pocket which is surrounded by a thin web. The pocket is fed with oil by capillaries which are connected to an oil pump (50 bar). The small gap h (typically in the range of 20 to 80 μm, Weck, 2002) between the web and the load m represents a hydraulic resistance R_h. Assuming: Newtonian fluid, laminar flow, a linear pressure drop over the web as shown in Fig. 1 (approximated by a constant pressure p_h effective up to the centre of the thin web), nearly static forces and motions, the pressure p_h can be calculated by the law of Hagen Poiseuille. An increasing pressure p_h respectively force F_h counteracts the external disturbance force F_{dis}. F_h can be determined with A_{eff}, the hatched area shown in Fig. 1 by

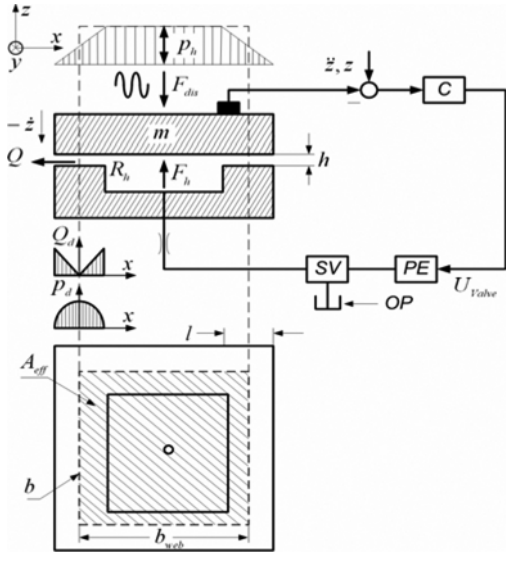

Fig. 1. Active Bearing with Control Loop.

Table 1. The Servo Valve Satisfies the Characteristics.

p_{supply}	50 bar
p_h	10 bar
f_{valve}	700 Hz
Q_{stat}	0,05
$Q_{dynamik}$	0-0,07 dm^3/min
$f_{operating}$	0 – 150 Hz

$$F_h = \frac{12 \cdot Q \cdot A_{eff} \cdot \eta \cdot l}{b \cdot h^3} \quad / \quad A_{eff} = b_{web}^2 \quad / \quad b = 4 \cdot b_{web} \tag{1}$$

To evaluate the characteristic parameters stiffness k and damping ratio d of a hydrostatic bearing it is meaningful to calculate their interdependence to the geometrical and material parameters of a single bearing. Denkena and Tönshoff (2005) derive a simplified relation for the damping Force F_d caused by an oscillating disturbance force F_{dis} under the assumption of p_d and Q_d as shown in Fig. 1.

$$d = \frac{F_d}{\dot{z}} = \frac{b \eta l^3}{h^3} \tag{2}$$

By neglecting hydraulic resistances (e.g. capillaries), keeping the flow rate constant ($F=F_0$), and an operating gap ($h=h_0-z$), a simplified equation (Weck, 2002) for the stiffness k can be derived using (1).

$$k = \frac{dF_h}{dz} = \frac{d\{F_h/F_0\}}{d\{z/h_0\}} \cdot \frac{F_0}{h_0} = \frac{36 \cdot Q_0 \cdot A_{eff} \cdot \eta \cdot l}{b \cdot h_0^4 \cdot (1 - z/h_0)^4} \tag{3}$$

Looking at (1) and (3), it is obvious that a further increase in the vibration control performance can be achieved by varying the flow rate Q. To achieve this, a torque motor servo valve is used as actuator. More about the function and construction of electro hydraulic servo valves can be taken from Will *et al.* (1999). The servo valve satisfies the characteristics shown in Table 1.

3. Testrig and plant modeling

The test rig in Fig. 2 consists of a hydrostatically

supported flexible beam and represents the cantilevered z-axis of a milling machine. The disturbance force $F_{process}$ corresponds to process forces, e.g. when a spindle operates on a work piece. The subsequent described investigations are performed as part of a research project funded by the German ministry for research and education (BMBF). Due to the research progress two different configurations of the test rig are investigated. This is concerning the effective direction of forces (x- and y-direction) as depicted in Fig. 2. During each configuration the remaining direction is not influenced actively.

The first configuration consists of two active bearings (two servo valves as actuators) in the x-direction at the top of the cantilevered beam and two passive bearings, so called "Schoenfeld Controllers." at the bottom (Fig. 2). Passive bearings are state-of-the-art and are used to increase the stiffness and the load bearing capacity, by keeping the gap h nearly constant. This is realized by a load-dependent restrictor. If the pressure in the pocket increases due to load changes, the flow rate Q respective counteracting pressure p_h increases too. For further theory and function of passive hydrostatic bearings it is referred to Weck (2002). As control variable the acceleration is measured at the tip of the cantilevered beam. In this case, the sensor is not placed at the point of the operating forces F_{h1x} and F_{h2x}, resulting in a non-collocation control problem. For simplicity the test rig is treated as a single-input-single-output (*SISO*) system, although there are two actuators F_{h1x} and F_{h2x}. Thereby, both actuators are supplied with the same white noise signal. The measured open plant frequency response function, from the servo valve drive voltage, to the acceleration at the tip of the beam, is depicted in Fig. 2, by the black solid line. As depicted by the grey line in Fig. 2, a sufficient model is obtained by manual model fitting. Due to the flexible systems properties and the strong phase loss up to the first two modes (*90 Hz* and *120 Hz*) this model will be used to design a robust μ-controller.

In the second configuration (y-direction, F_{hy}) the stiffness, reached by four passive bearings, will be compared with the achievable stiffness using four active bearings. In each case the bearings are equipped with magnetoresistive gap sensors (h_y).

The particularity in this y-configuration is that the opposite actuators, i.e. F_{h1y} and F_{h2y} respectively F_{h3y} and F_{h4y}, are driven by the same input signal, but for one actuator multiplied by *-1*. This so called double acting configuration is well known from the electromagnetic suspension of rotors. As control variables the averaged gaps of h_{1y} and h_{2y} (h_{12y}) respectively h_3 and h_4 (h_{34y}) are used. Beside the benefit of reducing a *4×4-MIMO*-system to two *SISO* decentralized control loops the double acting configuration has a linearising effect. To reveal this, the flow rate Q of two opposite actuators, e.g. F_{h1y}, F_{h2y}, is assumed to be constant Q_0. Simplified it can be taken from (1) that $F_h \sim Q_0/h^3$. With $Q_{h1}=Q_0+Q$ and $Q_{h2}=Q_0-Q$ respectively for the gaps $h_1=h_0+z$ and $h_2=h_0-z$ using (1) the resulting force $F_{hres}(h_0-z)$ is given by

$$F_{hres}(h_0-z) = F_{h1} - F_{h2} = \frac{2h_0\cdot\left(h_0^2+3z^2\right)}{\left(h_0^2-z^2\right)^3}\cdot Q - \frac{2Q_0\cdot\left(z^2+3h_0^2\right)}{\left(h_0^2-z^2\right)^3}\cdot z \qquad (4)$$

Figure 3 depicts this effect on $F_{hres}(h_0-z)$ by the black solid line, pointing out the approximately linear interval by the grey solid line. For comparison, the dash-dotted line shows the stronger nonlinear curve

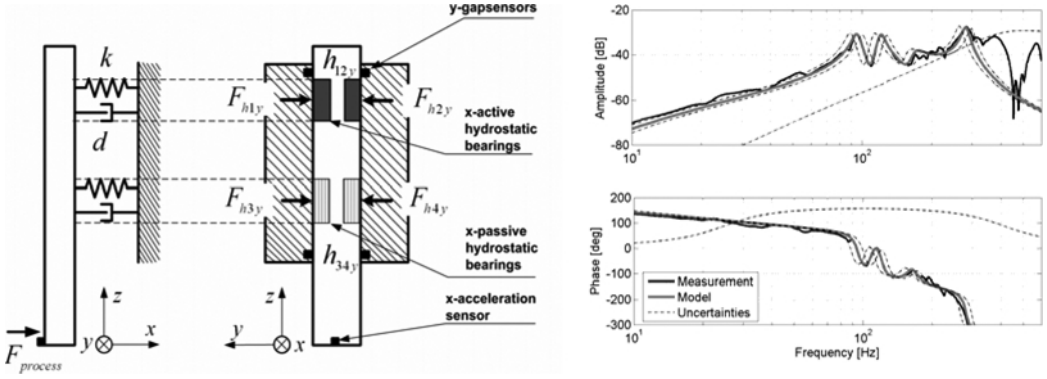

Fig. 2. Test rig (left) and Modelling of the Plant (right).

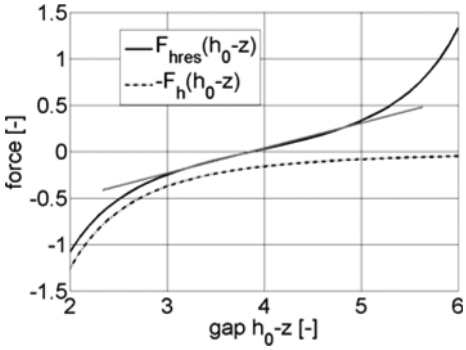

Fig. 3. Linearising Effect.

for a single hydrostatic bearing $-F_h(h_0-z)$.

4. μ-Controller design

For acceleration feedback a μ-controller will be designed. Therefore this section gives a brief summary of the elementary steps and equations in the μ-design procedure. For a more detailed description it is referred to Schönhoff (2003).

4.1 Uncertainty modeling of the plant

Additionally to the nominal model shown in Fig. 2 by the grey line, an uncertain model has to be set up. Two types of uncertainty, additive and parametric, are used. Additive uncertainty allows the consideration of neglected high frequency, flexible modes corresponding to the frequency band beyond *300 Hz* (Fig. 2). Parametric uncertainty in the natural frequencies ω enables the consideration of modelling errors, slight nonlinearities, or parameter changes which lead to a shift of the natural frequency. Mathematically this can be described by

$$G + \delta_a W_a \text{ and } \delta_\omega \Rightarrow \Delta = diag(\delta_a, \delta_\omega) \tag{5}$$

where Δ is the set of perturbations with δ_a for additive and δ_ω for parametric uncertainty. $W_a(s)$ is the frequency dependent amount of additive uncertainty. Finally this leads to the uncertain plant model $G_\Delta(s)$ depicted in Fig. 2 by the thin dashed lines.

4.2 Performance specification

In μ-synthesis the desired performance is specified in terms of bounds on the frequency response functions of a general closed control loop, depicted in Fig. 4. The relation between the outputs and the inputs of interest is given by

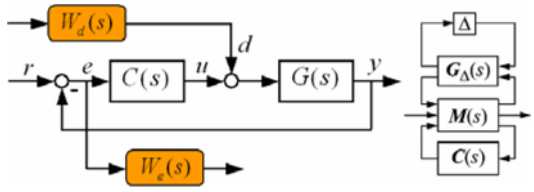

Fig. 4. General Control Loop and μ-Setup.

$$\begin{bmatrix} -e \\ u \end{bmatrix} = \begin{bmatrix} S & GS \\ -CS & -T \end{bmatrix} \cdot \begin{bmatrix} -r \\ d \end{bmatrix} \tag{6}$$

The objective is to achieve a high disturbance rejection e/d by minimizing and bounding the process sensitivity function GS. For a desired level of GS, it is further preferable to limit the corresponding control effort u/r, described by the control sensitivity function CS. The sensitivity function S also quantifies the disturbance rejection. The bound on the complementary sensitivity function T can not be chosen arbitrarily. It dependents on GS, CS, S, (Schönhoff, 2003). It can be taken from (6) that for realisation of the bounds on CS and GS at least two input signals r, d and two output signals e, u are required. Hence the bounds cannot be assigned directly to each frequency response function. The mathematically solution is to weight the four in- and outputs e, u, r, d by frequency dependent weighting functions W_r, W_d, W_e, W_u as depicted in Fig. 4, exemplary for W_d and W_e. The entire performance specification is expressed mathematically by the matrix M.

4.3 Synthesis and implementation of the μ-controller

The general setup for robust μ-controller synthesis in Fig. 4 is given by the interconnection

$$\boldsymbol{G} \circ \boldsymbol{M} \circ \boldsymbol{C} = \begin{bmatrix} W_e S W_r & W_e G S W_d \\ -W_u C S W_r & -W_u T W_d \end{bmatrix} \tag{7}$$

Using the D-K-Iteration of the Robust Control Toolbox (MATLAB), a controller of order 31 is synthesized and reduced to a lower order of 5 keeping the closed loop performance nearly constant. If the synthesized controller satisfies so that the well known H_∞-criterion (8) is fulfilled for all frequencies, it is given that the specified performance M will be achieved in reality with the μ-controller C, under the assumption that the real plant is covered by the uncertain model G_Δ. Hence the reciprocal values of the weighting functions W_r, W_d, W_e, W_u can be

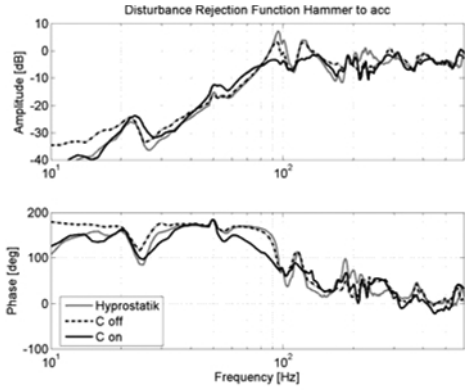

Fig. 5. FRF from hammer to acc.

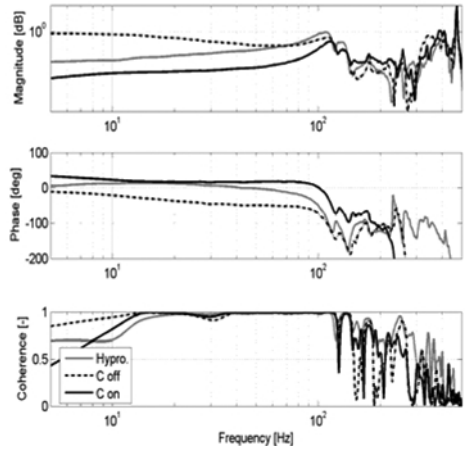

Fig. 6. FRF from hammer to h_{12y}.

interpreted as bounds for the sensitivity functions GS and CS (T, S analogous)

$$\|GMC\|_\infty \le 1 \;\Rightarrow\; |GS| \le |W_e W_d|^{-1} \text{ and } |CS| \le |W_u W_r|^{-1} \quad (8)$$

Finally, the controller C is discretized by using zero order hold transformation with a sample time of *5 kHz*, and implemented on a DSP.

5. Comparison and Results

For evaluation of disturbance rejection, frequency response functions (FRF) are measured from the hammer impulse to acceleration at the tip of the beam (Fig. 2). In Fig. 5 the results achieved with the passive controllers are depicted by the grey line. No damping effect of the first to modes at approx. *90 Hz* and *120 Hz* can be observed. This is obvious because the functionality and the inertial characteristic of the load dependent resistors are merely designed to increase the stiffness in the lower frequency range. As depicted by the black solid line the μ-controller and the active servo valves enable to achieve a damping ratio of approx. *7* to *9 dB* of the first two distinct modes. For comparison the dash-dotted line shows the active bearings when the controller is off. Fig.6 compares the stiffness of the active bearings with the stiffness of the passive bearings. In this case a simple *PI*-controller is sufficient. The frequency functions in Fig. 6 are calculated exemplary from hammer impulse to gap h_{12y}, an adequate measure for stiffness, when both control loops F_{12y} and F_{34y} are on. The line colours are retained corresponding to Fig. 5. The stiffness could be increased approx. factor 2 up to 90 Hz. Furthermore the third subplot in Fig. 6 shows the calculated coherence, which is a measure, how linear a signal is transferred to its response. Obviously a value of nearly 1 can be recognized down to 10 Hz. This holds for the effect described in the second section.

Conclusion

The experimental results clarify that vibration damping could be achieved with active hydrostatic bearings, using adequate control concepts, e.g. μ-synthesis. Anyhow, the effort spent for realisation is much higher than in the case of a simple proportional controller. Further research and investigations are necessary to transfer these results in the industrial applications, e.g. milling machines. The achievable performance has to be evaluated on a manufactured product and has to be traded off against the effort and higher complexity for realisation and maintenance.

References

Balas, G. J. and Doyle, J. C. 1994, "Robustness and Performance Trade-Offs in Control Design for flexible Structures," *IEEE Trans. In Control Systems Technology,* Vol. 2, No. 4.

Denkena, B. and Tönshoff, H., 2005, *Werkzeugmaschinen 1*. Vorlesungsskript - Institut für Fertigungstechnik und Werkzeugmaschinen, Hannover, Germany.

Hesselbach, J. and Gleichner, A., 1999, "Aktive hydrostatische Führungen mit elektrorheologischer Flüssigkeit – Neue Aktoren für intelligente Maschinen," *Zeitschrift für wirtschaftlichen Fabrik-betrieb,* **6**, 324~326.

Hesselbach, J. and Abel-Keilhack, Ch., 2002, "Active

Hydrostatic Bearing with Magnetorheological Fluid," *8th International Conference on New Actuators.* Bremen, Germany. pp. 343~346.

Preumont, A., 2002, *Vibration Control of Active Structures, an Introduction.* Kluver Academic Publishers, Dordrecht, The Netherlands.

Schönhoff, U., 2003, Practical Robust Control of Mechatronic Systems with Structural Flexibilities. Dissertation, Shaker-Verlag, Aachen, Germany.

Weck, M., 2002, *Werkzeugmaschinen, Fertigungssysteme Band 2 Konstruktion und Berechnung.* Springer-Verlag, Berlin, Heidelberg, Germany.

Will, D., 1999, *Hydraulik – Grundlagen, Komponenten, Schaltungen.* Springer-Verlag, Berlin, Heidelberg, Germany.